

Post-COVID ventilation design: Infection risk-based target ventilation rates and point source ventilation effectiveness

Jarek Kurnitski ^{a,b,*}, Martin Kiil ^a, Alo Mikola ^a, Karl-Villem Võsa ^a, Amar Aganovic ^c, Peter Schild ^d, Olli Seppänen ^e

^a Department of Civil Engineering and Architecture, Tallinn University of Technology, Tallinn, Estonia

^b Department of Civil Engineering, Aalto University, Espoo, Finland

^c Department of Automation and Process Engineering, UiT The Arctic University of Norway, Tromsø, Norway

^d Department of Built Environment, Oslo Metropolitan University, Oslo, Norway

^e Nordic Ventilation Group, Professor Emeritus, Aalto University, Espoo, Finland



ARTICLE INFO

Keywords:

Event reproduction number
Health-based ventilation
Virus removal
Pre-symptomatic period risk control
Air distribution
Tracer gas
Contaminant removal effectiveness
Air quality index

ABSTRACT

Ventilation, air filtration and disinfection have been found to be the main engineering measures to control the airborne respiratory infection transmission in shared indoor spaces. Wells-Riley model modifications allow to calculate the infection risk probability, but gaps in viral load data, risk control methods and dealing with incomplete mixing have resulted in ventilation recommendations falling short to consider activity and room specific viral loads and actual air distribution systems deviating from fully mixing. In this study a new infection risk-based ventilation design method operating with space category specific target ventilation rates and point source ventilation effectiveness is proposed. The method introduces the following novelties: i) explicit target ventilation rate equations depending on number of occupants and room volume derived for selected room categories ii) implementation of pre-symptomatic period infection risk control iii) point source ventilation effectiveness application to calculate the design ventilation rate for actual air distribution system iv) ventilation effectiveness measurement method with at least two point source locations developed and tested with laboratory and field measurements. Results show that in classrooms and offices existing Category I ventilation is enough in many cases, but higher ventilation is needed in meeting rooms, restaurants, and gyms where also occupancy reduction and advanced air distribution can be considered for feasible ventilation design.

1. Introduction

The impact of ventilation in reducing exposure to COVID-19 and other airborne respiratory infectious diseases has been widely discussed because SARS-CoV-2 and other respiratory pathogens have been shown to be effectively transmitted through the inhalation exposure route as concluded in the review by the Lancet COVID-19 Commission [1]. As a removal mechanism, outdoor air ventilation in buildings dilutes indoor-generated air pollutants (including bioaerosols) and reduces resulting exposures to occupants. Aerosol concentration reduction by ventilation applies for the long-range transmission, while short-range transmission occurs via face-to-face interactions in proximity to an infected person that clearly dominates at distances <1 m [2]. Ventilation and air cleaning, primarily designed to reduce long-range exposures, physical distancing, and mask wearing are four types of recommended aerosol

transmission control measures in many studies and guidelines [3]. Many recommendations to improve ventilation have been provided, but it is not easy to find an appropriate ventilation rate, because increasing ventilation has implications on energy use, CO₂ emissions, construction, and operation costs.

WHO [4] acknowledged the possibility of airborne transmission already in July 2020 by recognizing an increased risk of getting COVID-19 infection in crowded and poorly ventilated settings. WHO states that infected aerosols can remain suspended and improving indoor ventilation reduces the risk of the virus spreading indoors. Moreover WHO [5] has developed a roadmap to improve and ensure good indoor ventilation in the context of COVID-19 that is divided into three settings – health care, non-residential and residential spaces. In this study we focus on the ventilation design in non-residential buildings, where WHO recommends 10 L/s per person minimum ventilation rate with reference to EN

* Corresponding author at: Department of Civil Engineering and Architecture, Tallinn University of Technology, Tallinn, Estonia.

E-mail address: jarek.kurnitski@ttu.ee (J. Kurnitski).

16798-1:2019 [6]. This value is recommended as the highest, Category I value defined in the existing standard. Beyond existing standards, an effective air change rate of 4–6 ACH has been proposed by Allen and Ibrahim [7] to reduce long-range airborne transmission of SARS-CoV-2 by targeting this air change rate through any combination of outdoor air ventilation, recirculated air passing through effective filter, or passage of air through portable air cleaner. Their recommendation is justified with inhalation dose risk reduction and is intended for large group of indoor spaces such as classrooms, retail shops, and homes if guests are visiting. Obviously, this recommendation does not distinguish spaces with low and high occupant density and has energy and cost implications because the ventilation rates proposed are close to ones used in health care buildings. While virus removal by high ventilation rates and physical distancing to avoid the close contact can be relatively easily organised in non-residential spaces, the situation is different in residential buildings. Typical ventilation rates of 0.5 ACH in homes are much lower and it is difficult to avoid the close contact that makes it difficult to control the infection risk.

Epidemiological study by Buonanno et al. suggests that ventilation rates from 10 to 14 L/s per student reduced the likelihood of infection for students by 80% compared with a classroom relying only on natural ventilation [8]. However, in this study airflow rates were not measured and were estimated based on typical values measured for naturally ventilated classrooms in the previous study, and on design specification of installed new single classroom ventilation units. Measuring air change in 10 441 classrooms included in the study would have meant a massive measurement effort showing a challenge to get epidemiological evidence. High infection risk in naturally ventilated classrooms with low air change rate is also reported by Schibuola and Tambani [9]. The Lancet COVID-19 Commission [1] reviewed the scientific evidence around ventilation and disease transmission for SARS-CoV-2 and other airborne pathogens and found that there is coalescence around ventilation targets above current minimums. Based on this assessment, they propose 10, 14 and > 14 L/s per person non-infectious air delivery rates corresponding to 4, 6 and > 6 ach as good, better, and best ventilation levels.

For all these recommendations it is common that no calculation method is provided for infection risk control. While L/s per person ventilation values may work both for spaces with low and high occupant density, highly different viral loads of breathing, speaking and physical activities [10] must be considered in the ventilation design. Another aspect is that recommendations are for well-mixed conditions and the effect of air distribution deviating from fully mixing cannot be taken into account. The latter is important because an infector acts as point source in the room and zones with different virus concentration may easily be formed. Therefore, the ventilation need will depend on ventilation effectiveness and advanced air distribution solutions may be used to reduce the required ventilation rate and virus concentration in the breathing zone [11]. Thus, existing recommendations fall short of recognizing the hazard of airborne respiratory infection transmission and, in turn, the necessity of risk control.

The problem is that currently there is no method available for non-residential setting to design building ventilation and other measures to protect occupants against respiratory disease transmission at reasonable risk level. The current design of ventilation according to existing indoor climate standards EN 16798-1:2019 [6] and ISO 17772-1:2017 [12] has been limited to the use of ventilation criteria based on the perceived air quality (odours) depending on emissions from humans and a building and on specific pollutant concentration control. This approach neglects respiratory disease transmission for which the key engineering measure is ventilation, supported if necessary with air filtration or air disinfection [13]. It should be noted that Milton showed already in 2000 that lower levels of outdoor ventilation were associated with increased short term sick leave [14], but this has never been implemented in ventilation design methods. Policy recommendation by Morawska et al. [15] emphasizes the need to develop the standards to explicitly consider infection control in their stated objectives.

First steps towards infection risk-based ventilation design method are taken in [16] introducing a ventilation rate equation derived from Wells-Riley model modification that allows to calculate the required ventilation at given infection risk probability for fully mixing air distribution in the steady state. The risk control concept introduced, used the event reproduction number, enabling to consider the number of occupants, room volume, and filtration and portable air cleaners as other removal mechanisms in the calculation of required ventilation rate. Federspiel et al. [17] has proposed the same equation with extension of the reproduction number from single event to full pre-symptomatic period.

This study presents an infection risk-based ventilation design method which takes into account viral loads of different activities in typical indoor spaces as well as the effects of actual air distribution methods deviating from fully mixed conditions through ventilation effectiveness concept. Infection risk is controlled by considering the number of occupants and setting the reproduction number of the pre-symptomatic period to $R_0 = 1$ with an assumption that the likelihood of infecting others is constant during the total interaction time with susceptible persons. SARS-CoV-2 quanta emission data reported in the review by Aganovic et al. [18] and ventilation equation by Kurnitski et al. [16] have been used to derive new, space category specific target ventilation rate equations valid for fully mixed air distribution. To calculate the design ventilation rate to be supplied by ventilation system, a new test method for the point source ventilation effectiveness measurement was developed to take into account the actual air distribution system and varying concentration in the room. The design method includes calculation of ventilation rates with existing perceived air quality-based ventilation design method, and finally selection the highest ventilation rate of two methods as a design ventilation rate.

2. Methodology

This study consists of the following steps to develop a new infection risk-based ventilation design method:

1. Ventilation rate equation at given infection risk probability for fully mixing air distribution in the steady state [16] is used as a starting point. This Wells-Riley model modification provides an explicit equation for the ventilation rate and has two important input parameters: the quanta emission rate and individual infection risk probability. The rest of input parameters are straightforward, considering occupancy, room volume and other removal mechanisms than ventilation. The main limitation for the application is the value of individual infection risk probability, which is impossible to define because the target is not to control an individual infection but the spread of epidemic in population. Therefore, the infection risk control concept is extended in step 3.
2. Quanta emission rates from the latest review [18] are used as input data to define the scenario based on measured median viral load. As the viral load is a parameter with large variation, we have opted only for selecting representative quanta values for the purpose of adequate ventilation in shared indoor spaces. If the purpose is to model an event with a super spreader, extremely high values are to be used. In our application, the aim is not to eliminate, but reduce the infection risk: an infectious person should infect no more than one person during the pre-symptomatic period; therefore median values of the viral load are justified to use.
3. Infection risk control concept based on basic reproduction number $R_0 = 1$ during pre-symptomatic infectious period accounting all possible out-of-home interactions with susceptible persons. For this purpose, it is assumed that the likelihood of infecting others (i.e. the number of infections per unit time) is constant over the pre-symptomatic infectious period allowing to calculate the event reproduction number depending on the length of occupancy in a specific space. While pre-symptomatic infectious period ends at the

onset of symptoms, it is assumed that infector self-isolates and is not any more in contact with susceptible individuals. Thus, the risk control concept does not cover symptomatic period. With this risk control concept, an individual probability value for a specific room, fulfilling $R_0 = 1$, can be calculated. This allows to derive a space category specific target ventilation rate Q equation as a function of number of persons (N) and room volume (V) for fully mixing air distribution.

4. While in many settings air distribution may differ from fully mixing, the ventilation rate needs to be adjusted based on ventilation effectiveness of actual air distribution. EN 16798-3:2017 [30] defines ventilation effectiveness as contaminant removal effectiveness, more specifically the air quality index for the breathing zone that is calculated as the ratio between the extract air concentration and average concentration in the breathing zone. This existing ventilation effectiveness concept commonly used with distributed source (=pollutants from all occupants) is applied with a point source corresponding to an infector and is also compared with air change efficiency. The latter compares the time it actually takes to replace the air in the room to shortest possible air change time. For actual air distribution solution, the point source ventilation effectiveness ϵ_b measurement method is developed to calculate the infection risk-based design ventilation rate Q_s supplied by ventilation system.
5. Finally, infection risk-based design ventilation rate Q_s needs to be compared with perceived air quality-based ventilation rate q_s that is calculated with EN 16798-1:2019 [6] and ISO 17772-1:2017 [12] method.
6. The highest value of q_s and Q_s is selected as the design ventilation rate.

The developed design method is tested with point source ventilation effectiveness ϵ_b measurements in the classroom mock up and field measurements in a large teaching space and meeting room. Design ventilation rate calculation for typical rooms is conducted. The method is applicable for long-range airborne transmission; thus, close proximity is to be avoided, for which 1.0–1.5 m distancing can be recommended [19]. In principle the method is independent from ventilation system type and can be applied for mechanical, hybrid or natural ventilation systems.

3. Infection-risk based ventilation rate

3.1. Infection risk control concept

Kurnitski et al. [16] used Wells-Riley model modification to derive an explicit equation for ventilation rate in the steady state at given infection risk probability and fully mixing air distribution:

$$Q = \frac{(1 - \eta_i)IqQ_b(1 - \eta_s)D}{\ln(\frac{1}{1-p})} - (\lambda_{dep} + k + k_f + k_{UV})V \quad (1)$$

where

Q outdoor air ventilation rate (m^3/h)

p probability of infection for a susceptible person (-)

q quanta emission rate per infectious person (quanta/(h pers))

Q_b volumetric breathing rate of an occupant (m^3/h)

I number of infectious persons (-)

η_s facial mask efficiency for a susceptible person (-)

η_i facial mask efficiency for an infected person (-)

D duration of the occupancy (h)

λ_{dep} deposition onto surfaces (1/h)

k virus decay (1/h)

k_f filtration by a portable air cleaner (1/h)

k_{UV} disinfection by upper room ultraviolet germicidal irradiation UVGI (1/h)

V volume of the room (m^3)

The main parameters affecting the required ventilation rate are the quanta emission rate (=emission source intensity), occupancy duration, accepted level of probability of infection, room volume and other removal mechanisms in addition to outdoor air ventilation, such as air cleaners, UVGI or facial masks. If a portable air cleaner is used, the filtration removal rate (k_f) is calculated based on the airflow rate through the filter (Q_f), the removal efficiency of the filter (η_f), and room volume V :

$$k_f = \frac{Q_f \eta_f}{V} \quad (2)$$

For portable cleaners with a high-efficiency particle air (HEPA) filter, the clean air delivery rate (CADR, m^3/h) [20] can be used to calculate the filtration removal rate as $k_f = CADR/V$. The removal efficiency of filters and the CADR are particle-size dependent. These parameters can be estimated based on the size range of 0.3–0.5 μm [21].

An acceptable individual probability p for a specific room, corresponding to basic reproduction number $R_0 = 1$, can be calculated based on the event reproduction number R , defined as the number of new disease cases divided by the number of infectors $R = N_c/I$. Considering that the number of new cases $N_c = p N_s$ an acceptable individual probability for a specific room can be calculated as follows:

$$p = \frac{RI}{N_s} = \frac{RI}{(N - I)(1 - f_v \eta_v)} \quad (3)$$

where

R event reproduction number (-)

N_s the number of susceptible persons in the room, $N_s = N - I$ if no vaccinated/immune persons

f_v fraction of the local population who are vaccinated, $f_v = 0$ for no vaccination (-)

η_v the efficacy of the vaccine against becoming infectious, $\eta_v = 1$ for ideal protection (-)

Acceptable R during one room-occupancy event can be based on the assumption that the likelihood of infecting others (i.e. the number of infections per unit time) is approximately constant over the pre-symptomatic infectious period. If it can be ensured that the R in each event is below 1, the pre-symptomatic infectious period R_0 would be less than 1 no matter what schedule people follow in different indoor environments [22]. In such cases, an infectious person will not infect more than one person during the pre-symptomatic infectious period. Therefore, the exposure can be integrated over events by introducing an average interaction time [1] between infector and susceptible occupant during the infectious period:

$$\frac{R}{R_0} \cong \frac{D}{D_{inf}} \implies R \leq \frac{D}{D_{inf}} \text{ when } R_0 \leq 1 \quad (4)$$

where:

R event reproduction number, i.e. number of people who become infected per infectious occupant

D room occupancy period, i.e. length of time when both infectious and susceptible persons are present in the room at the same time (h)

D_{inf} the total interaction time when an infectious individual is in the vicinity of any susceptible persons during the whole pre-symptomatic infectious period (h)

R_0 basic reproduction number that describes the spread of an epidemic in the population (-)

The pre-symptomatic infectious period of about 2½ days ends typically at the onset of symptoms when the infectious person self-isolates at home or is otherwise ‘removed’ from contact with susceptible individuals. For example, if an infectious person is in the vicinity of susceptible persons (e.g. on public transport, at work/school) for 20 h altogether during the pre-symptomatic infectious period, then he or she must not infect more than $R = 1/20 = 0.05$ persons per hour, on average, in order to remain within the limit of $R_0 \leq 1$.

It is possible to simplify Equation (1) by using the Taylor

Table 1

Estimated quanta-RNA relationship for various strains of SARS-CoV-2.

	RNA quanta	Virus variant quanta multiplier (-)
Original (Wuhan)	14,000	1.0
Alpha (B.1.1.7)	7400	1.9
Delta (B.1.617.2)	5000	2.8
Omicron (B.1.1.529)	1200	11.7

Table 2

Average quanta emission rates (quanta/h) for SARS-CoV-2 original strain.

Buonanno et al. 2020	Aganovic et al. 2023	Aganovic et al. 2023
Viral load	Viral load	Viral load
10^7 RNA/mL	10^7 RNA/mL	10^8 RNA/mL
(66th percentile value)	(35th percentile value)	(56th percentile value)
Breathing	0.72	0.01
Speaking	9.7	0.38
Singing	62	0.90
		0.13
		3.8
		9.0

approximation of an exponential $e^n \cong 1 + n$ at low doses that allow for the rewriting as follows:

$$\frac{1}{1-p} = e^{\frac{(1-\eta_s)qQ_b(1-\eta_s)D}{(\lambda_{dep}+k+k_f+k_{UV})V}} \quad (5)$$

Taylor approximation provides reasonable accuracy at low p values, for instance, 2.4% at $p = 0.05$ and 4.7% at $p = 0.1$. By using another approximation $1/(1-p) \cong 1+p$ that applies if $|p| \ll 1$, and substituting R from Equation (6), Equation (5) can be solved for ventilation rate Q as follows:

$$Q = \frac{(1-\eta_s)qQ_b(1-\eta_s)DN_s}{R} - (\lambda_{dep} + k + k_f + k_{UV})V \quad (6)$$

This equation enables us to calculate infection-risk-based ventilation rates in a simple fashion when substituting default values of quanta emission rate, breathing rate, and occupancy duration. If no face masks are being worn and ventilation is the only removal mechanism Equation (6) simplifies:

$$Q = \frac{qQ_bDN_s}{R} - (\lambda_{dep} + k)V \quad (7)$$

3.2. SARS-CoV-2 quanta emission values and breathing rates

In Aganovic et al. [23] review SARS-CoV-2 quanta emission rates derivation from viral RNA has been reported. He used six size ranges of aerosol droplet diameter to calculate the total dry volume of aerosols per litre of exhaled breath during various respiratory activities such as breathing, speaking, and singing. Viral RNA in different-sized respiratory aerosols emitted by infected patients measured by Coleman et al. [24] was used to calculate the viral copies contained in fine dehydrated aerosols. For the viral load in the sputum, an average viral load of $10^{8.1}$ RNA/mL was used, which is close to the median viral load for non-vaccinated (median $10^{8.1}$ RNA/mL) and vaccinated individuals (median $10^{7.8}$ RNA/mL) [25].

Table 3

Time averaged breathing rates and quanta emission rates (56th percentiles). The term ‘10% speaking’ means that infected individuals speak 10% of the time on average.

	Breathing rate Q_b , m ³ /h	SARS-CoV-2 original	Delta variant	Omicron variant
Classroom, infected student 5% speaking	0.57	0.31	0.9	3.7
Office work, 10% speaking	0.60	0.50	1.4	5.8
Restaurant, 20% speaking	0.65	0.86	2.4	10.1
Meeting, 20% speaking	0.65	0.86	2.4	10.1
Sport, 50% heavy exercise, 50% resting	1.92	0.51	1.4	5.9

Table 4

Volumetric breathing rates.

	Breathing rate Q_b , m ³ /h
Default sedentary activity, non-speaking	0.54
Talking	1.10
Light exercise	1.38
Heavy exercise	3.30

Table 5Virus specific ventilation parameters q_q and q_r in Equation (8).

Space category	q_q , L/(s person)	q_r , L/(s m ³)
Classroom	10	0.24
Office	23	0.24
Assembly hall	30	0.24
Meeting room	40	0.24
Restaurant	40	0.24
Gym	70	0.24

The quanta-RNA relationship $1\text{ quanta} = 14 \cdot 10^3$ RNA copies have been derived by [18] based on human challenge data studies [26] and [27] reported for a wild pre-alpha variant. Based on the quanta-RNA relationship for the original Wuhan strain, the quanta-RNA for several successive strains can be defined [18] as shown in Table 1.

When comparing the quanta-emission rates (quanta/h) proposed by Buonanno et al. [10], there are differences more than tenfold even for the same expiratory activities and viral load [18], as shown in Table 2. This significant difference is caused by the difference between the values used to describe the quanta-RNA relationship. Buonanno used 200 viral copies based on data for SARS-CoV-1, compared to 14,000 viral copies of the original SARS-CoV-2 strain.

Quanta emission rate values at viral load 10^8 RNA/mL for Delta and Omicron variants can be calculated as shown in Table 3 by applying the virus variant multipliers from Table 1 and considering typical time averages of speaking and breathing activities. In the similar fashion, time-averaged volumetric breathing rates depending on the activity [28] being undertaken, are calculated from values shown in Table 4.

3.3. Infection-risk based target ventilation rates for fully mixing air distribution

Quanta emission and breathing rates derived in Table 3 allow to substitute the values for typical occupied spaces to Equation (7) that will simplify to space category specific target ventilation rate equation

$$Q = q_q(N - 1) - q_r V \quad (8)$$

where

Q target outdoor air ventilation rate (L/s)

q_q quanta emission specific ventilation rate for occupancy per person (L/(s person))

q_r removal rate of virus decay and deposition (L/(s m³))

N the number of persons in the room

V room volume (m³)

The first term of Equation (8) represents the quanta emission specific ventilation rates qq depending only on viral load and risk level and is

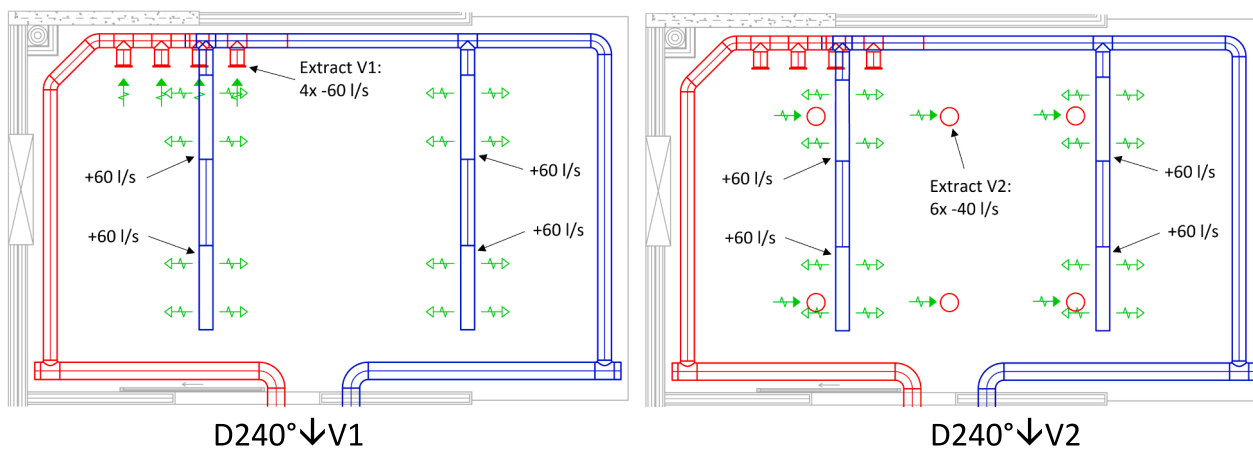


Fig. 1. Air distribution systems with duct diffusers. D240°↓V1 has four extract air devices in one corner of the classroom ceiling and D240°↓V2 has six ceiling extracts.

therefore possible to be recalculated also for other respiratory viruses. The second term q_r represents removal mechanisms by deposition and virus decay which is also virus specific parameter. In the case of portable air cleaners and ultraviolet disinfection, another removal term ($k_f + k_{UV}$) V/3.6 has to be added as it follows from Equation (6). The following default values have been applied to establish a scenario to calculate q_q and q_r values reported in Table 5:

- surface deposition loss rate $\lambda_{dep} = 0.24 \text{ 1/h}$ [10]
- virus decay $k = 0.63 \text{ 1/h}$ [29]
- quanta emission rate time average values calculated in Table 3 for Omicron, i.e. $q = 4 \text{ quanta/(h pers)}$ in classrooms, $6 \text{ quanta/(h pers)}$ in offices and gyms, and $10 \text{ quanta/(h pers)}$ in meeting rooms and restaurants
- number of infectious persons in the room $I = 1 \text{ pers}$
- breathing rate time averaged values reported in Table 3
- occupancy duration $D = 2, 6, \text{ and } 9 \text{ h}$ in meeting rooms, classrooms, and offices, respectively
- interaction time of an infectious individual in the vicinity of susceptible persons, including traveling, lunches, and other out-of-home activities, $D_{inf} = 22.5 \text{ h}$ in offices and 16 h in schools over 2.5 days of the pre-symptomatic infectious period

Infection-risk based target ventilation rates calculated with Equation (8) can be compared with EN 16798-1:2019 [6] and ISO 17772-1:2017 [12] perceived air quality-based ventilation rate:

$$q_{tot} = Nq_p + A_R q_B \quad (9)$$

where

q_{tot} total outdoor air ventilation rate for the breathing zone (L/s)

N design value for the number of persons in the room

q_p ventilation rate for occupancy per person (L/(s person))

A_R room floor area (m^2)

q_B ventilation rate for emissions from building (L/(s m^2))

4. Infection-risk based design ventilation rates for actual air distribution

4.1. Point source ventilation effectiveness

Target outdoor air ventilation rates calculated using the equations (8) and (9) apply at fully mixing air distribution. An actual air distribution solution may deviate from fully mixing so that lower or higher quanta concentrations will form to the breathing zone. So far, there have been two modelling approaches to account for the mixing conditions by

utilizing the concept of ventilation effectiveness that can be determined using measured tracer gas concentrations:

$$\varepsilon_v = \frac{C_e - C_o}{C_i - C_o} \quad (10)$$

where

ε_v ventilation effectiveness as defined in EN 16798-3:2017 [30], contaminant removal effectiveness in Rehva Guidebook No 2 [31] (-)

C_e concentration in the extract air duct

C_i average concentration at the breathing level

C_o concentration in the supply air

Previous studies have shown that the tracer gases, such as CO_2 used in this study, can be used as reliable predictor for the exposure to aerosol particles [32]. Shen et al. [33] applied ventilation effectiveness to the removal rate of the ventilation meaning that other removal mechanisms will be calculated with average quanta concentration considered to be equal across the space. This results in ventilation rate supplied by actual air distribution system:

$$q_s = \frac{q_{tot}}{\varepsilon_v} \quad (11)$$

Aganovic et al. [23] applied ventilation effectiveness in the multi-zone model where the space under consideration is typically divided horizontally or vertically into two perfectly mixed zones with uniform quanta concentrations in each zone. Airflows between the zones are described with mixing factor for which the expression as a function of the ventilation effectiveness has been derived. This approach with complicated equations allows to account different quanta concentration in each zone and will lead to more accurate results. However, Aganovic et al. [18] has shown that the differences are marginal and Equation (11) provides plausible results if ventilation is dominating removal mechanism.

Important limitation of ventilation effectiveness ε_v , not considered before, is the determination from an average concentration at the breathing level and measurement with distributed tracer gas source [31], that describes contaminant emission from all occupants in the room. In the case of one infector, the situation is different and corresponds to point source typically with many possible locations in the room. To be suitable to describe an infector, we propose the point source ventilation effectiveness (contaminant removal effectiveness measured with a point source) for the breathing zone, to be calculated as an average of two or more tracer gas measurements with different source locations. We also propose that concentrations of not all measurement points in the room, but only 50% of measurement points with the highest concentration are accounted for in measurement with each

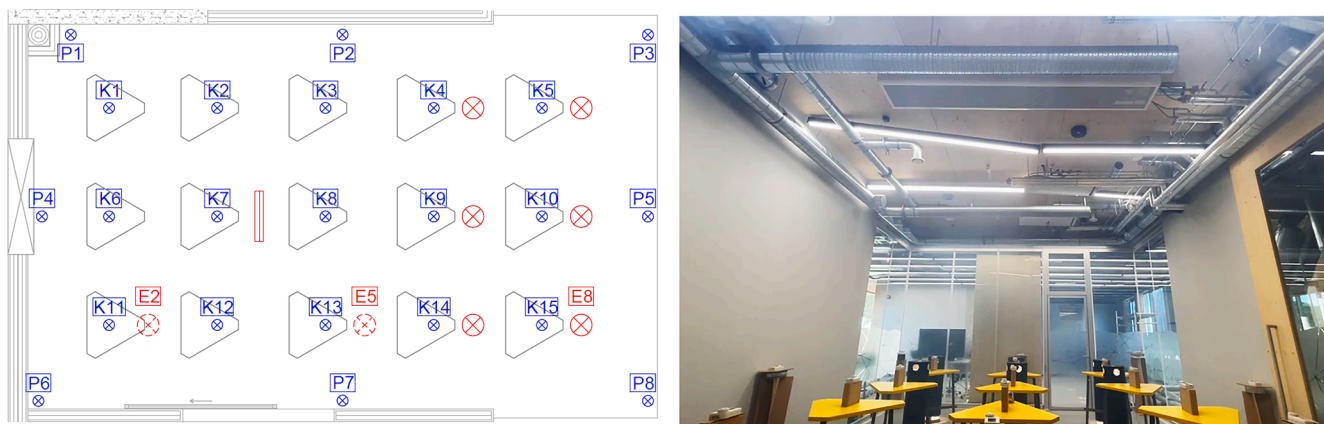


Fig. 2. Location of the measurement points and a photo of the mock-up room. Breathing plane measurement points K1–K15 at 1.1 m height, source positions E2, E5, and E8, and perimeter measurement points P1–P8 for illustrative purposes.

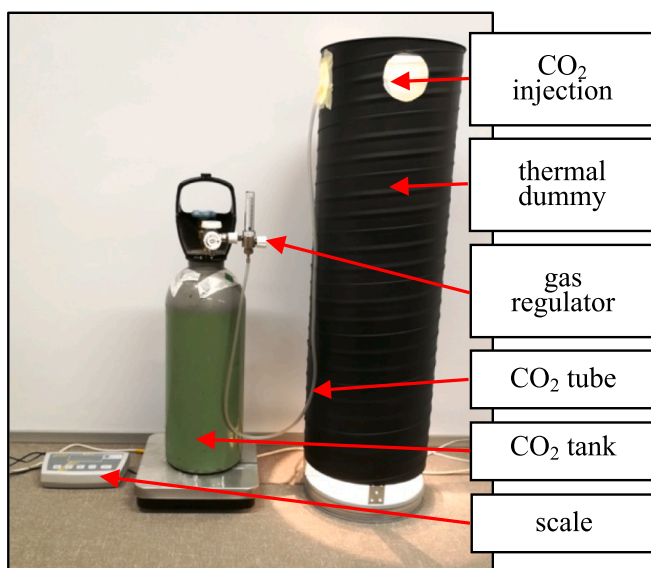


Fig. 3. CO₂ bottle connected to a dummy used as a contaminant source.

source location j:

$$\varepsilon_b^j = \frac{C_{je} - C_{jo}}{C_{jb} - C_{jo}} \quad (12)$$

$$\varepsilon_b = \frac{\sum \varepsilon_b^j}{m} \quad (13)$$

where

ε_b^j point source ventilation effectiveness of measurement with source location j

ε_b point source ventilation effectiveness for the breathing zone

C_{je} measurement j concentration in the extract air duct

C_{jb} measurement j concentration at the breathing level that is calculated as an average concentration of 50% of the measurement points having the highest concentrations

C_{jo} concentration in the supply air

m total number of measurements with different point source locations

Proposed 50% of the measurement points rule was found as practical consideration in measurements. In many cases the distribution of tracer gas in the room was highly uneven and large clean zones with

very low concentration formed. Closer to the source, concentrations were remarkably higher. Therefore, calculating the average value provided much lower concentration than it was a real exposure for many occupants located closer to the source. Accounting only 50% of measurement points with the highest measured concentrations provides a safety margin to overcome this problem especially in large rooms. In small rooms with relatively even concentration difference this calculation rule practically did not affect the results. Therefore, for an actual air distribution solution, the ventilation rate Q_s to be supplied by the ventilation system can be calculated as follows:

$$Q_s = \frac{Q}{\varepsilon_b} \quad (14)$$

where

Q target ventilation airflow rate for the breathing zone from equation 8 (L/s)

Q_s design ventilation airflow rate at actual air distribution solution (L/s)

ε_b point source ventilation effectiveness for the breathing zone (-)

4.2. Point source ventilation effectiveness measurements in the laboratory

Two air distribution systems with duct diffusers, as shown in Fig. 1, were measured to test the point source ventilation effectiveness measurement method. The local air quality index measurement procedure specified in Rehva Guidebook No 2 [31] was followed, in an open-ceiling mock-up classroom with a room height of 3.8 m and floor area of 5.2 × 8.7 m (45 m²). Both cases had duct diffusers with downward and side nozzles (240°). In the case of D240°↓V1, extract air devices were installed in one corner of the ceiling and D240°↓V2 had six equally distributed extracts on the ceiling. A ventilation rate of 240 L/s (5.3 L/(s m²), 5 l/h), supply air temperature of 18 °C, and room temperature of 22 °C were used in all measurements.

Three locations of point source E2, E5, and E8, as shown in Fig. 2, were measured. These locations were selected not from the middle of the room but from the desk row to have a longer distance to extract air devices. CO₂ as a tracer gas with a continuous dose method according to ISO 12569:2017 [34] was used. CO₂ concentrations were measured at breathing plane ($h = 1.1$ m), from supply air duct and extract air duct.

Tracer gas was injected continuously during the test by using a CO₂ bottle connected to a heated dummy as a contaminant source (Fig. 3). Inside the dummy, the tracer gas tube was directed downwards to achieve good mixing, and it was ensured that no tracer gas was released from the bottom opening of the dummy. Therefore, the plume of the dummy released mixed tracer gas to the room from upper openings.

For comparison, air change efficiency was also measured, which was done using the concentration decay method. Air change efficiency is

Table 6

Average of local air quality index $\bar{\varepsilon}_P$ (K1-K15), point source ventilation effectiveness for each measurement ε_b^j calculated with 50% of measurement points rule and as average of three measurements ε_b , and air change efficiency ε^a for two studied air distribution systems.

	$\bar{\varepsilon}_P$, -	ε_b^j , -	ε_b , -	ε^a , %
D240°↓V1, E2 source	1.09	1.02		
D240°↓V1, E5 source	0.95	0.87		
D240°↓V1, E8 source	0.90	0.82		
D240°↓V1			0.91	56
D240°↓V2, E2 source	1.10	1.03		
D240°↓V2, E5 source	1.28	1.00		
D240°↓V2, E8 source	1.15	0.98		
D240°↓V2			1.00	50

defined as $\varepsilon^a = \tau_n/2\tau$, where τ_n is nominal time constant and τ is the room mean age of air. In this case, the tracer gas was released to a room and mixed well with a fan before the decay measurement was conducted.

The local air quality index was calculated for each measurement

point K1–15 as follows:

$$\varepsilon_P = \frac{C_e - C_o}{C_p - C_o} \quad (15)$$

where

ε_P local air quality index at the measurement point P

C_p steady state concentration at the measurement point P

Measurement points closer than 1.5 m to the source were excluded. Calculation of indices is reported in [Appendix A Tables A1 and A2](#) and summarised in [Table 6](#). Results show that point source ventilation effectiveness calculated from 50% of the points with the lowest values are slightly lower than an average of local air quality index. Ventilation effectiveness ε_b was calculated as an average of results from three locations of the source. It can be also seen that if only two source locations E5 and E8 would have been used, ε_b would get slightly lower values of 0.85 and 0.99 respectively due to more unfavourable source locations.

To illustrate the concentration distributions in the room, the local air quality index values were plotted, as shown in [Fig. 4](#). These can be compared with air change efficiency values ε_a , which apply for distributed source and the concentration decay method ([Fig. 5](#)). It can be seen,

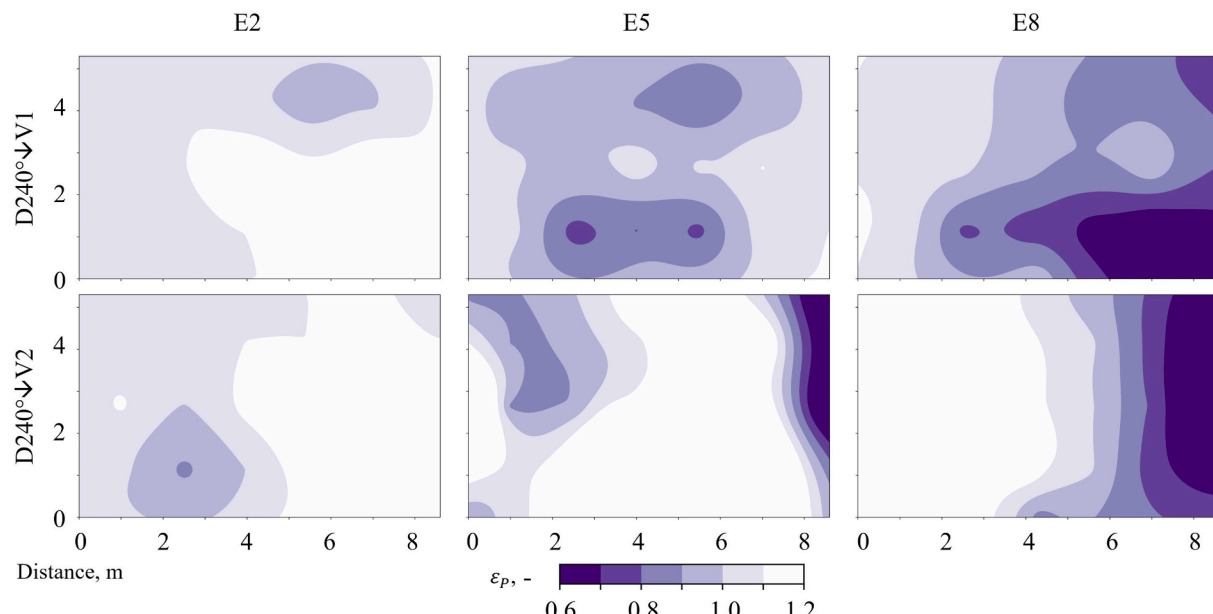


Fig. 4. The distribution of local air quality index values with three locations of point source. The point source ventilation effectiveness $\varepsilon_b = 0.91$ for D240°↓V1 and $\varepsilon_b = 1.00$ for D240°↓V2.

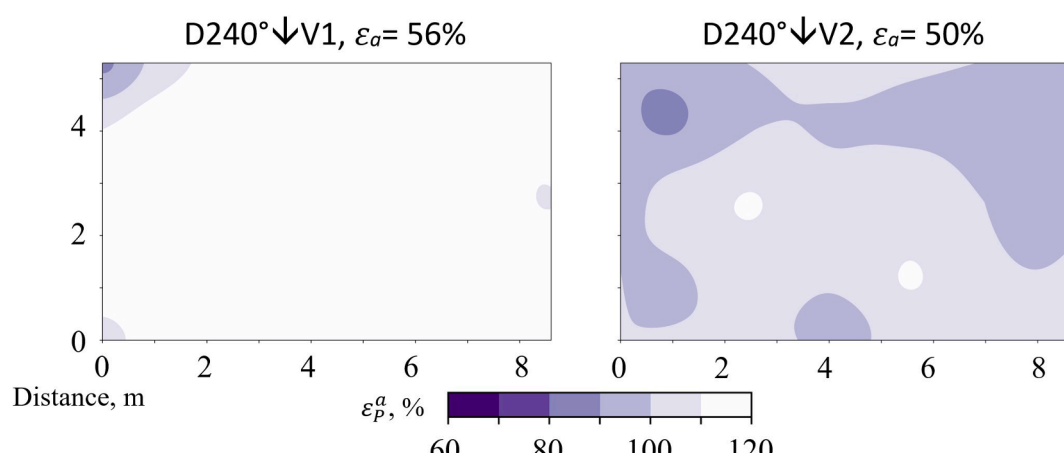


Fig. 5. Air change efficiency values and the distribution of local air change index values.

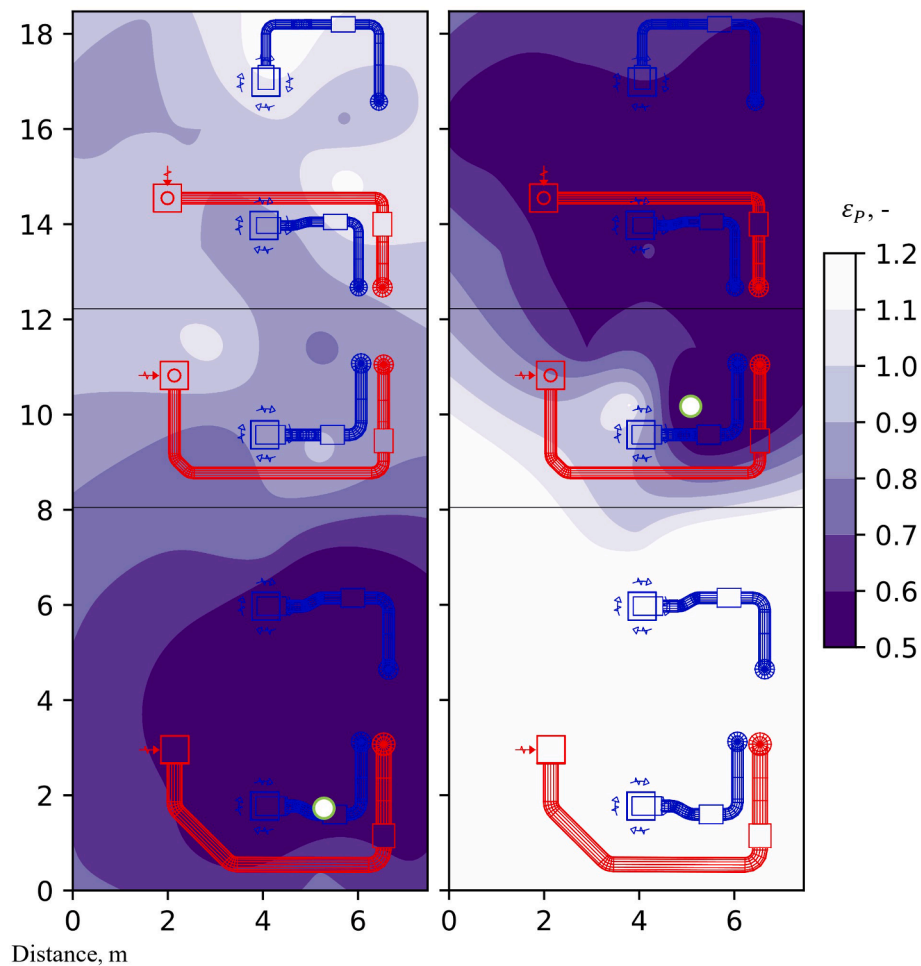


Fig. 6. Local air quality index values with two locations of point source in the large teaching space of 130 m^2 with $4 \text{ L}/(\text{s m}^2)$ ventilation. Emission source is marked with green/white circle. Point source ventilation effectiveness values $\varepsilon_b^1 = 0.66$ (left) and $\varepsilon_b^2 = 0.53$ (right) and the average value of two measurements $\varepsilon_b = 0.60$. (For interpretation of the references to colour in this figure legend, the reader is referred to the web version of this article.)

Table 7

Average of local air quality index $\bar{\varepsilon}_p$, point source ventilation effectiveness for each measurement ε_b^j and as average of two measurements ε_b in the teaching space.

	$\bar{\varepsilon}_p$, -	ε_b^j , -	ε_b , -
Source in one end	0.82	0.66	
Source in centre	1.19	0.53	
Ventilation effectiveness			0.60

that D240°↓V1 achieved a higher air change efficiency (56%) than that of D240°↓V2 (50%), which corresponds exactly to fully mixing air distribution. It is important to see that fully mixing air distribution with distributed source is not necessarily a fully mixing with point source, as is the case with D240°↓V1. Despite achieving 56% air change efficiency, this air distribution system produces a lower value for the point source ventilation effectiveness (0.91). At the same time, D240°↓V2 with multiple extract points has resulted in fully mixing both with distributed and point source ($\varepsilon_a = 50\%$, $\varepsilon_v = 1.00$ and $\varepsilon_b = 1.00$).

4.3. Point source ventilation effectiveness measurements in large rooms

Field measurements were conducted in large spaces which cannot be measured in the laboratory. The same procedure as in the laboratory was used with two source location to measure local air quality index with continuous dose method. In Fig. 6, the results from a large teaching

space of 130 m^2 are shown. This teaching space with room height of 2.9 m consisted of three classrooms with movable partitions. In the measurement it was one open space for 50 persons. There were 5 supply air ceiling diffusers and 3 extract air diffusers with total outdoor ventilation rate of 520 L/s . Tracer gas measurements were conducted with 3×9 measurement points equally distributed on 1.1 m height. Additionally, 3 extract air concentration measurements were conducted from which airflow weighted average extract air concentration was calculated. Outdoor air concentration was measured from supply air duct.

Results show that high concentration zone forms around the emission source. While in the left Fig. 6 (emission source in one end of the space) the concentration is reasonably equally distributed, the right Fig. 6 with the centre of the room source location has resulted in high concentration zone in one end of the room and low concentration zone in another end. In this low concentration zone, local air quality index values were as high as 2.7 showing that calculation of ε_b^2 as an average value of all points would result in 1.19 instead of $\varepsilon_b^2 = 0.53$ calculated with 50% of measurement points rule, Table 7. In the left Fig. 6 this difference is smaller, 0.82 instead of $\varepsilon_b^1 = 0.66$ respectively. Relatively low value of $\varepsilon_b = 0.60$ indicates that with a point source, fully mixing cannot be expected in large rooms.

The effect of extract air devices' location can be seen from 24-person meeting room measurements, Fig. 7. In this room with 52.5 m^2 floor area and 2.7 m height, 3×4 concentration measurement points were used from 1.1 m height and one measurement from extract air duct. Chilled beams with $3 \text{ L}/(\text{s m}^2)$ ventilation rate have resulted in reasonably well-

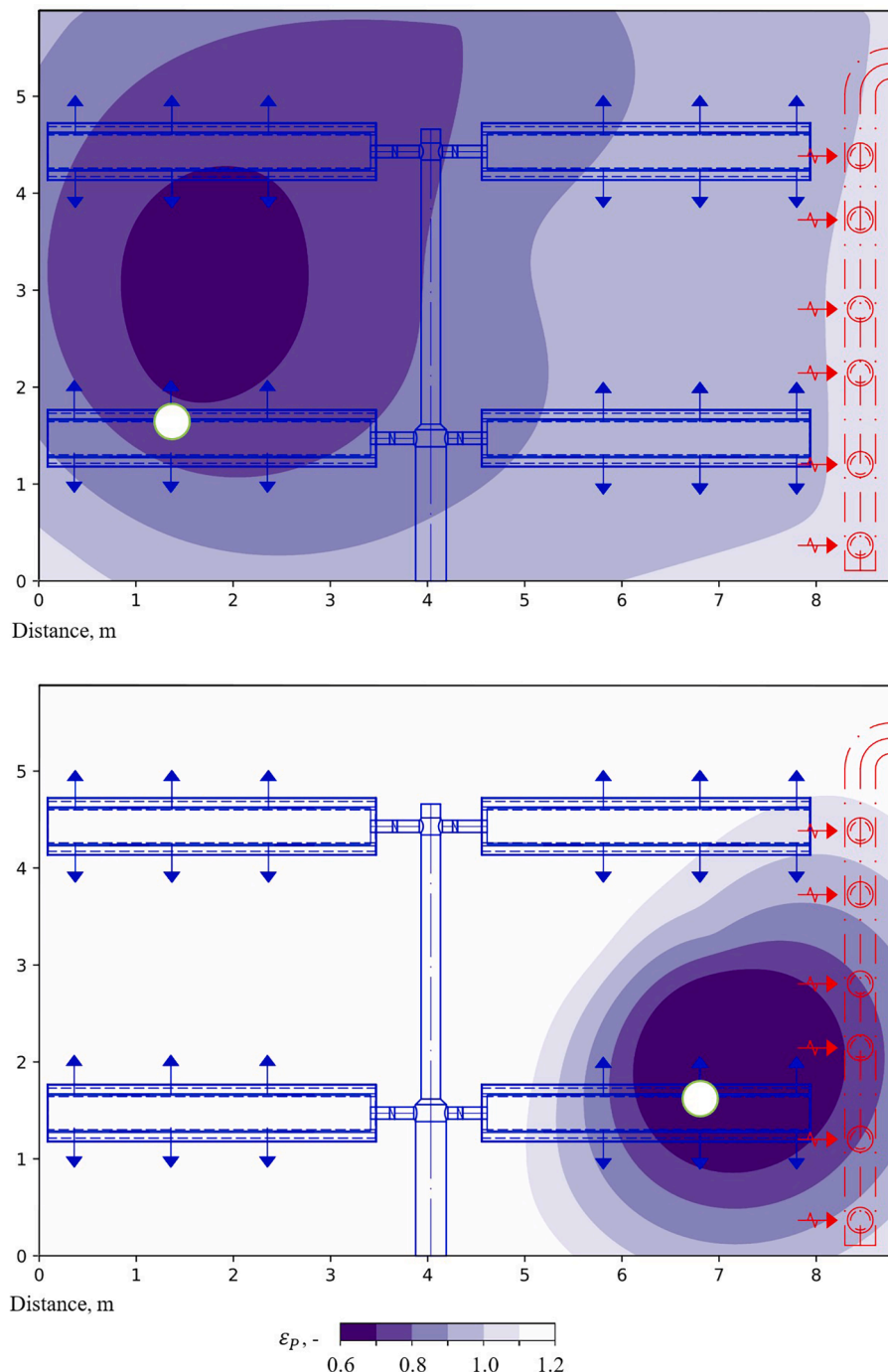


Fig. 7. Local air quality index values with left and right locations of point source in the meeting room of 52.5 m^2 with $3.0 \text{ L/(s m}^2\text{)}$ ventilation. Emission source is marked with green/white circle. (For interpretation of the references to colour in this figure legend, the reader is referred to the web version of this article.)

Table 8

Average of local air quality index $\bar{\varepsilon}_p$, point source ventilation effectiveness for each measurement ε_b^l and as average of three measurements ε_b in the meeting room.

	$\bar{\varepsilon}_p$, -	ε_b^l , -	ε_b , -
Left source	0.87	0.79	
Centre source	0.88	0.80	
Right source	1.44	1.11	
Ventilation effectiveness			0.90

mixed condition in the case of the left source location that is far from extract air devices. In this case, local air quality index values range 0.7–1.0 in most of the room area. In the case of the right source location close to extract air devices, the situation is completely different so that high concentration zone forms close to the source and in the white area in the figure, local air quality index values range 1.5–2. Point source ventilation effectiveness values are shown in Table 8.

5. Calculated airflow rates for some rooms

The application of Infection-risk-based ventilation rate equation (8) is illustrated using calculation examples for typical spaces in Table 9.

Table 9

Calculation example of health- and comfort-based ventilation rates in typical rooms. Infection-risk-based ventilation rates are calculated using equation (8) and Category II and I comfort ventilation with Equation (9). CO₂ concentration is calculated from the infection-risk-based ventilation rate with ε_v = 1.00.

	Floor	Room	No of	Infection-risk-based ventilation			Comfort ventilation			
	area	height	persons	Ventilation effectiveness	Ventilation rate	Ventilation rate	Air change rate	CO ₂ conc.	Cat. II ventilation	Cat. I ventilation
	m ²	m	N, -	ε _b , -	L/(s pers)	L/(s m ²)	1/h	ppm	L/(s m ²)	L/(s m ²)
Classroom	42.5	2.9	25	0.91	9.2	5.4	6.7	941	4.8	6.9
Classroom	56.5	2.9	25	0.90	8.9	3.9	4.9	962	3.8	5.4
reduced occ.	56.5	2.9	20	0.90	8.4	3.0	3.7	999	3.2	4.5
Large teaching space	129.5	2.9	50	0.60	13.3	5.1	6.4	776	3.4	4.9
reduced occ.	129.5	2.9	40	0.60	12.5	3.8	4.8	801	2.9	4.1
2-person office	21.0	2.6	2	1.00 ¹	4.9	0.5	0.6	1535	1.4	2.0
Open-plan office	56.7	2.6	6	0.80 ¹	16.5	1.7	2.4	736	1.4	2.1
Open-plan office	173.0	2.6	17	0.60	25.4	2.5	3.5	619	1.4	2.0
Meeting room	29.2	2.6	10	1.00	34.2	11.7	16.2	563	3.1	4.4
reduced occ.	29.2	2.6	6	1.00	30.3	6.2	8.6	584	2.1	3.1
Meeting room	52.5	3.2	24	0.90	40.7	18.6	20.9	536	3.9	5.6
reduced occ.	52.5	3.2	12	0.90	37.0	8.5	9.5	550	2.3	3.3
Restaurant	259.5	2.9	154	0.60 ¹	64.3	38.1	47.3	486	4.9	6.9
reduced occ.	259.5	2.9	50	0.60 ¹	59.3	11.4	14.2	494	2.0	2.9
Gym	173.5	3.5	12	0.60	86.5	6.0	6.2	657		
School gym	217.5	6.0	25	0.50	109.1	12.5	7.5	604		

¹ not measured, assumed value.

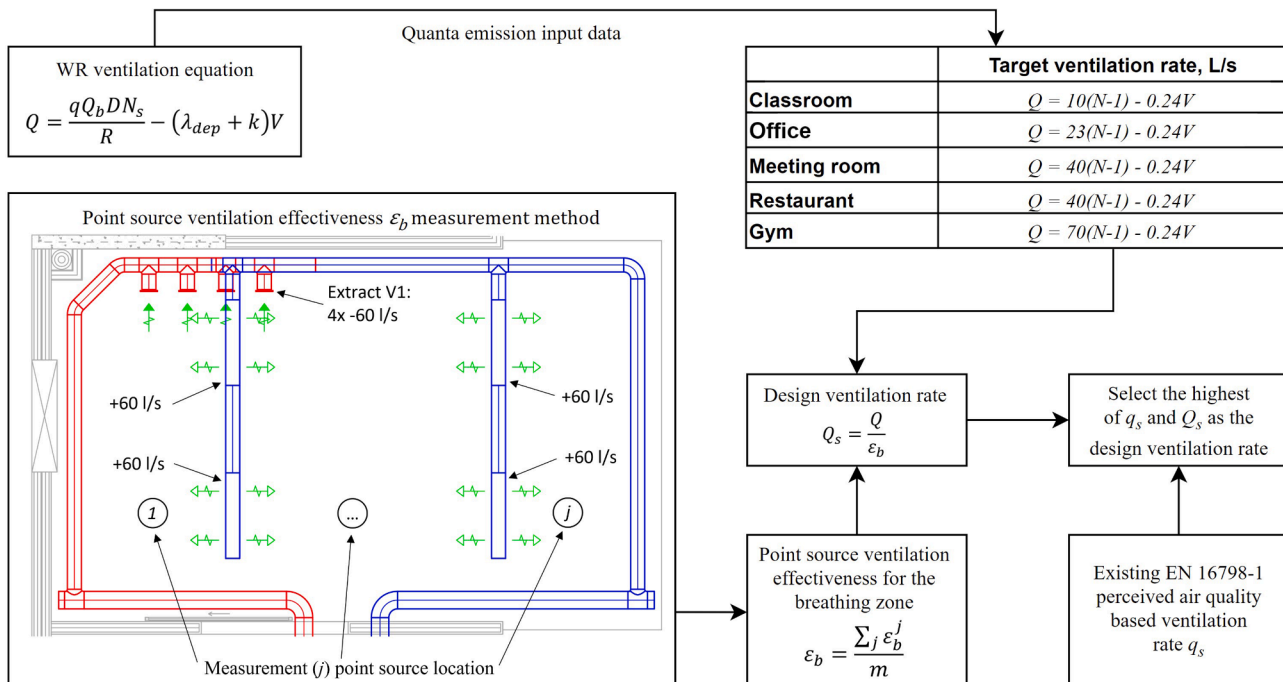


Fig. 8. Main steps in the application of the ventilation design method.

Infection-risk-based ventilation rates are calculated as L/s per person and floor area as well as air change rates for selected rooms. These values are then compared with Category I and II (EN 16798-1:2019 [6]) ventilation rates, calculated with equation (9) with the assumption of low-polluting building materials as follows:

- 10 L/s per person + 1 L/s per floor area in Category I;
- 7 L/s per person + 0.7 L/s per floor area in Category II.

In the case of Category I and II ventilation rates, fully mixing air distribution is assumed ($\epsilon_v = 1.0$) because, in this case, instead of one infector/point source, all occupants emit pollutants (human bio effluents and CO₂). Therefore, the emission source is equally distributed and fully mixing can be expected also in large rooms with common mixing

ventilation solutions.

In the infection-risk-based ventilation rate calculation, point source ventilation effectiveness values either measured or estimated for typical mixing ventilation solutions are used. CO₂ concentrations are calculated using an outdoor concentration of 400 ppm and CO₂ generation rates of 18 L/h in classrooms, 20 L/h in offices, meeting rooms, and restaurants and 80 L/h in the gym which correspond to typical metabolic rates in such spaces [35].

In classroom and office cases, which are highlighted in Table 9, Category I and Category II ventilation rates are higher than infection-risk-based ventilation rates. In meeting rooms and restaurants, the airflow rates are high even with reduced occupancy, indicating that these rooms require air distribution solutions with higher ventilation effectiveness to achieve a feasible ventilation design. However, in such

Table A1

The local air quality index calculated from measurement results.

	D240°↓V1			D240°↓V2		
	E2 source	E5 source	E8 source	E2 source	E5 source	E8 source
K1	1.05	0.96	1.01	1.09	0.90	1.51
K2	1.10	0.98	1.03	1.06	0.95	1.29
K3	1.01	0.89	0.96	1.10	1.07	1.13
K4	0.94	0.82	0.85	1.10	1.27	1.03
K5	0.99	0.93	0.87	1.23	1.30	0.76
K6	1.04	1.02	1.10	1.11	0.88	1.58
K7	1.10	1.00	1.03	1.00	0.92	1.40
K8	1.23	1.06	0.94	1.14	1.16	1.13
K9	1.12	1.01	0.89	1.24	1.16	1.02
K10	1.21	1.10	0.98	1.29	1.22	0.78
K11	1.04	1.04	1.07	1.02	1.08	1.46
K12	1.04	0.76	0.78	0.88	1.25	1.25
K13	1.10	0.80	0.76	1.00	2.03	1.20
K14	1.18	0.77	0.65	1.15	2.31	1.02
K15	1.11	1.04	0.57	1.14	1.63	0.75
AVG K1-K15	1.09	0.95	0.90	1.10	1.28	1.15

Table A2

Calculation of point source ventilation effectiveness ε_p .

	D240°↓V1			D240°↓V2		
	E2 source	E5 source	E8 source	E2 source	E5 source	E8 source
0.94	0.76	0.65	0.88	0.88	0.76	
0.99	0.77	0.76	1.00	0.90	0.78	
1.01	0.82	0.78	1.00	0.92	1.02	
1.04	0.89	0.85	1.06	0.95	1.02	
1.04	0.93	0.87	1.09	1.07	1.03	
1.05	0.96	0.89	1.10	1.08	1.13	
1.10	0.98	0.94	1.10	1.16	1.13	
1.10	1.00	0.96	1.11	1.16	1.20	
1.10	1.01	0.98	1.14	1.22	1.25	
1.11	1.02	1.01	1.14	1.25	1.29	
1.12	1.04	1.03	1.15	1.27	1.40	
1.18	1.04	1.03	1.23	1.30	1.46	
1.21	1.06	1.07	1.24	1.63	1.51	
1.23	1.10	1.10	1.29	2.31	1.58	
Average of 50% of measurement points with lowest values	1.02	0.87	0.82	1.03	1.00	0.98
Average of 2 (E5 and E8) source locations		0.85			0.99	
Average of 3 source locations		0.91			1.00	

rooms, a 1.0–1.5 m distance requirement will lead roughly to 50% occupancy (every second seat empty); therefore, the ventilation rates shown in the Table 9 with normal occupancy are not needed and just represent a theoretical case.

6. Discussion

Infection risk-based ventilation rates may be higher than comfort ventilation rates, as shown in Table 9, but are required only during epidemic periods. In normal conditions – that is, outside of epidemic periods – a demand-controlled operation is recommended to comply with comfort-based values and to optimise the energy used for ventilation [36]. For energy considerations, the ventilation operation mode can

be automatically changed from infection risk-based ventilation to demand-controlled if a low occupancy threshold is set. This should correspond to number of persons at which the lower limit of ventilation rate is sufficient according to Equation (14). It is shown by Wang et al. [37] that occupant density can be detected based on video frames from surveillance cameras, that is more responsive method than CO₂ monitoring and offers a new possibility to integrate occupant density to ventilation control. Demand-controlled ventilation systems can be forced to constant air volume operation at nominal fan speed by changing CO₂ setpoint to 550 ppm as recommended in [36].

The application of the developed design method is illustrated in Fig. 8. Calculation of the target ventilation rate is straightforward, the only data needed is the number of occupants and the room volume. It

should be noted that this is valid for the scenario established with default value assumptions in section 3.3. Because quite many occupancy, virus and viral load related parameters are needed, there is clear standardisation need to find representative values for realistic scenario definition.

The target ventilation applies at the breathing zone and to find the design ventilation rate to be supplied by the ventilation system, the point source ventilation effectiveness ϵ_b , taking into account the actual air distribution method, is needed. This is challenging for practical application because such data is currently not available even for commonly used air distribution methods. Some values exist for ventilation effectiveness ϵ_v measured with distributed contaminant source as defined in EN 16798-3:2017 [30]. ϵ_v values are provided in CEN/TR 16798-4:2017 [38], ASHRAE 62.1:2022 [39] and in air distribution method reviews by Cao et al. [40] and Yang et al. [41]. Yalin et al. [42] showed an example of CFD application to analyse ventilation effectiveness indices in a hospital room. However, ϵ_v values cannot be used for ϵ_b that has to be measured with point source to describe the situation with one infector in the room.

Application of the measurement method proposed in this paper showed that further guidance how to locate the tracer gas source during measurements would be needed to be developed, because this may have remarkable effect on results. Even how the source is introduced is not standardised, and the direction and momentum of the tracer gas injection may have impact on mixing with room air. On the other hand, limiting the method to long range transmission with 1.0–1.5 m distancing makes it slightly less sensitive to source description in close proximity, but some air distribution solutions such as displacement ventilation may be highly sensitive for stratification and on upward or downward movement of injected tracer gas. Currently we recommend using one position with worse possible location, i.e., with longest distance to extract typically in one end or corner of the occupied zone, and other positions with more central or typical occupant locations. However, the positions directly below extract air devices should not be used to avoid local exhaust effect which may lead to too optimistic results. Practical considerations limit the number of source positions to 2–3 because one measurement with continuous dose of tracer gas will need about three-time constants to stabilise and then a short period to record the data. A 50% of the measurement points with highest concentration calculation -rule is also ad-hoc proposal which needs further development. Therefore, future studies could apply CFD and statistical analyses to further study and refine methodology for the point source ventilation effectiveness measurement.

7. Conclusions

In this study, new infection risk-based ventilation design method was developed intended to complement an existing perceived air quality-based design method in EN 16798-1:2019 [6] and ISO 17772-1:2017 [12] standards. The following conclusions can be drawn:

- Target ventilation rate equation (8) depending only on number of occupants and room volume was derived by considering activities and corresponding median viral load in selected room categories, valid in the steady state and fully mixing conditions.
- It was shown that infection risk control results in paradigm change in air distribution design. Current principle of effective removal of contaminants from distributed sources (normal occupancy) is changed to removal of contaminants from the point source (infector) with many possible locations in the breathing zone.
- Methodology was developed for point source ventilation effectiveness measurement enabling to calculate the design ventilation rate for actual air distribution system. This method is applicable also in large rooms and is based on tracer gas measurements at least with two source locations.

- In 42.5 m² classroom it was possible to achieve fully mixing both with distributed and point source, resulting in air change efficiency of 50% and point source ventilation effectiveness of 1.0. In 130 m² teaching space with mixing ventilation, concentration differences formed and decreased the point source ventilation effectiveness to 0.6 showing that air change efficiency cannot be used to describe ventilation efficiency.
- As a final step, new design method includes calculation with existing perceived air quality based EN 16798-1:2019 [6] and ISO 17772-1:2017 [12] ventilation design method to select the highest ventilation rate of two methods as a design ventilation rate to be supplied by the ventilation system.
- In typical classrooms and offices, infection risk-based ventilation rates (Table 9), following the assumed scenario's and related default values, mostly did not exceed Category I perceived air quality-based ventilation rates, ranging in classrooms 8–13 L/s per person.
- In meeting rooms, restaurants and gyms, infection-risk based ventilation rates (Table 9) were remarkably high, indicating that feasible ventilation design would need an advanced air distribution and reduced occupancy.

CRediT authorship contribution statement

Jarek Kurnitski: Conceptualization, Methodology, Supervision, Writing – original draft. **Martin Kiil:** Formal analysis, Investigation, Writing – original draft. **Alo Mikola:** Formal analysis, Investigation, Data curation. **Karl-Villem Võsa:** Formal analysis, Investigation, Visualization. **Amar Aganovic:** Conceptualization, Methodology, Formal analysis. **Peter Schild:** Conceptualization, Methodology, Formal analysis. **Olli Seppänen:** Conceptualization, Methodology, Writing – review & editing.

Declaration of Competing Interest

The authors declare that they have no known competing financial interests or personal relationships that could have appeared to influence the work reported in this paper.

Data availability

Data will be made available on request.

Acknowledgements

Estonian Centre of Excellence in Zero Energy and Resource Efficient Smart Buildings and Districts, ZEBE (grant 2014-2020.4.01.15-0016) funded by the European Regional Development Fund, EU Horizon 2020 SmartLivingEPC project (Grant Agreement number: 101069639) and Finnish Government's analysis, assessment, and research project ILMIRA, have supported this research. Nordic Ventilation Group and REHVA Technology and Research Committee COVID-19 Task Force are greatly acknowledged for support to develop this ventilation design method.

Appendix A

The local air quality index calculated with Equation (15) for two studied air distribution systems with three locations of the point source (2x3 = 6 measurements) is shown in Table A1. An average of all measurement points is calculated for illustrative purposes (ventilation effectiveness according to Equation (10)). Measurement points that are closer than 1.5 m to the source are highlighted.

The calculation of point source ventilation effectiveness is presented in Table A2. Measurement points closer than 1.5 m to the source (highlighted in Table A1) are excluded and all other values are sorted in ascending order. From 50% of the points with the lowest values

(highlighted in Table A2), an average is calculated. Finally, ventilation effectiveness ϵ_b is calculated as an average of results from three locations of the source.

References

- [1] The Lancet COVID-19 Commission Proposed Non-infectious Air Delivery Rates (NADR) for Reducing Exposure to Airborne Respiratory Infectious Diseases. November 2022.
- [2] J. Wagner, T.L. Sparks, S. Miller, W. Chen, J.M. Macher, J.M. Waldman, Modeling the impacts of physical distancing and other exposure determinants on aerosol transmission, *J. Occup. Environ. Hyg.* 18 (2021) 495–509.
- [3] T.C. Bond, A. Bosco-Lauth, D.K. Farmer, P.W. Francisco, R.J. Pierce, K.M. Fedak, J. M. Ham, S.H. Jathar, S. VandeWoude, Quantifying proximity, confinement, and interventions in disease outbreaks: a decision support framework for air-transported pathogens, *Environ. Sci. Technol.* 55 (2021) 2890–2898.
- [4] World Health Organization Coronavirus disease (COVID-19): Ventilation and air conditioning, 23 December 2021 Available online: <https://www.who.int/news-room/questions-and-answers/item/coronavirus-disease-covid-19-ventilation-and-air-conditioning>.
- [5] World Health Organization Roadmap to improve and ensure good indoor ventilation in the context of COVID-19; World Health Organization: Geneva PP - Geneva, 2021; ISBN 9789240021280 (electronic version).
- [6] CEN EN Standard, 16798-1. Energy performance of buildings—Ventilation for buildings—Part 1: Indoor environmental input parameters for design and assessment of energy performance of buildings addressing indoor air quality, *Therm. Environ. Light. Acoust.* (2019).
- [7] J.G. Allen, A.M. Ibrahim, Indoor air changes and potential implications for SARS-CoV-2 transmission, *Jama* 325 (2021) 2112–2113.
- [8] G. Buonanno, L. Ricolfi, L. Morawska, L. Stabile, Increasing ventilation reduces SARS-CoV-2 airborne transmission in schools: A retrospective cohort study in Italy's Marche region, *Front. Public Heal.* 10 (2022) 4922.
- [9] L. Schibulka, C. Tambani, High energy efficiency ventilation to limit COVID-19 contagion in school environments, *Energy Build.* 240 (2021), 110882.
- [10] G. Buonanno, L. Morawska, L. Stabile, Quantitative assessment of the risk of airborne transmission of SARS-CoV-2 infection: prospective and retrospective applications, *Environ. Int.* 145 (2020), 106112.
- [11] W. Su, B. Yang, A. Melikov, C. Liang, Y. Lu, F. Wang, A. Li, Z. Lin, X. Li, G. Cao, Infection probability under different air distribution patterns, *Build. Environ.* 207 (2022), 108555.
- [12] ISO Standard. 17772-1:2017 Energy performance of buildings - Indoor environmental quality - Part 1: Indoor environmental input parameters for the design and assessment of energy performance of buildings.
- [13] L. Morawska, J.W. Tang, W. Bahnfleth, P.M. Bluyssen, A. Boerstra, G. Buonanno, J. Cao, S. Dancer, A. Floto, F. Franchimon, How can airborne transmission of COVID-19 indoors be minimised? *Environ. Int.* 142 (2020), 105832.
- [14] D.K. Milton, P.M. Glencross, M.D. Walters, Risk of sick leave associated with outdoor air supply rate, humidification, and occupant complaints, *Indoor Air* 10 (2000) 212–221.
- [15] Morawska, L.; Allen, J.; Bahnfleth, W.; Bluyssen, P.M.; Boerstra, A.; Buonanno, G.; Cao, J.; Dancer, S.J.; Floto, A.; Franchimon, F. A paradigm shift to combat indoor respiratory infection. *Science (80-)*. 2021, 372, 689–691.
- [16] J. Kurnitski, M. Kiil, P. Wargocki, A. Boerstra, O. Seppänen, B. Olesen, L. Morawska, Respiratory infection risk-based ventilation design method, *Build. Environ.* 206 (2021), 108387.
- [17] Fedderspiel, C.; Azimi, P.; Stephens, B.; Wargocki, P. An Air Quality Operating Guideline for the COVID-19 Pandemic and Beyond. In Proceedings of the Healthy Buildings 2021 Conference; 2022.
- [18] A. Aganovic, G. Cao, J. Kurnitski, P. Wargocki, New dose-response model and SARS-CoV-2 quanta emission rates for calculating the long-range airborne infection risk, *Build. Environ.* 228 (2023), 109924.
- [19] P.V. Nielsen, C. Xu, Multiple airflow patterns in human microenvironment and the influence on short-distance airborne cross-infection—A review, *Indoor Built Environ.* 31 (2022) 1161–1175.
- [20] American National Standards Institute (ANSI) ANSI/AHAM AC-1-2020 Method For Measuring Performance Of Portable Household Electric Room Air Cleaners.
- [21] REHVA Criteria for room air cleaners for particulate matter. Recommendation from the Nordic Ventilation Group. 2021 Available online: <https://www.rehva.eu/>
- [22] Y. Guo, N. Zhang, T. Hu, Z. Wang, Y. Zhang, Optimization of energy efficiency and COVID-19 pandemic control in different indoor environments, *Energy Build.* 261 (2022), 111954.
- [23] A. Aganovic, G. Cao, J. Kurnitski, A. Melikov, P. Wargocki, Zonal modeling of air distribution impact on the long-range airborne transmission risk of SARS-CoV-2, *Appl. Math. Model.* 112 (2022) 800–821.
- [24] Coleman, K.K.; Tay, D.J.W.; Tan, K. Sen; Ong, S.W.X.; Than, T.S.; Koh, M.H.; Chin, Y.Q.; Nasir, H.; Mak, T.M.; Chu, J.J.H. Viral load of severe acute respiratory syndrome coronavirus 2 (SARS-CoV-2) in respiratory aerosols emitted by patients with coronavirus disease 2019 (COVID-19) while breathing, talking, and singing. *Clin. Infect. Dis.* 2022, 74, 1722–1728.
- [25] R. Costa, B. Olea, M.A. Bracho, E. Albert, P. de Michelena, C. Martínez-Costa, F. González-Candela, D. Navarro, RNA viral loads of SARS-CoV-2 Alpha and Delta variants in nasopharyngeal specimens at diagnosis stratified by age, clinical presentation and vaccination status, *J. Infect.* 84 (2022) 579–613.
- [26] R. Sender, Y.M. Bar-On, S. Gleizer, B. Bernshtain, A. Flamholz, R. Phillips, R. Milo, The total number and mass of SARS-CoV-2 virions, *Proc. Natl. Acad. Sci.* 118 (2021).
- [27] B. Killingley, A.J. Mann, M. Kalinova, A. Boyers, N. Goonawardane, J. Zhou, K. Lindsell, S.S. Hare, J. Brown, R. Frise, Safety, tolerability and viral kinetics during SARS-CoV-2 human challenge in young adults, *Nat. Med.* 28 (2022) 1031–1041.
- [28] B. Binazzi, B. Lanini, R. Bianchi, I. Romagnoli, M. Nerini, F. Gigliotti, R. Duranti, J. Milic-Emili, G. Scano, Breathing pattern and kinematics in normal subjects during speech, singing and loud whispering, *Acta Physiol.* 186 (2006) 233–246.
- [29] N. Van Doremalen, T. Bushmaker, D.H. Morris, M.G. Holbrook, A. Gamble, B. N. Williamson, A. Tamin, J.L. Harcourt, N.J. Thornburg, S.I. Gerber, Aerosol and surface stability of SARS-CoV-2 as compared with SARS-CoV-1, *N. Engl. J. Med.* 382 (2020) 1564–1567.
- [30] CEN EN Standard. 16798-3. Energy performance of buildings - Ventilation for buildings - Part 3: For non-residential buildings. *Perform. Requir. Vent. room-conditioning Syst. (Modules M5-1, M5-4)* 2017.
- [31] Mundt, M.; Mathisen, H.M.; Moser, M.; Nielsen, P. V Ventilation effectiveness: Rehva guidebooks. 2004.
- [32] M. Bivolarova, J. Ondráček, A. Melikov, V. Ždímal, A comparison between tracer gas and aerosol particles distribution indoors: The impact of ventilation rate, interaction of airflows, and presence of objects, *Indoor Air* 27 (2017) 1201–1212.
- [33] J. Shen, M. Kong, B. Dong, M.J. Birnkrant, J. Zhang, A systematic approach to estimating the effectiveness of multi-scale IAQ strategies for reducing the risk of airborne infection of SARS-CoV-2, *Build. Environ.* 200 (2021), 107926.
- [34] ISO/TC 163; CEN/TC 89 ISO 12569:2017 Thermal performance of buildings and materials. *Determ. Specif. airflow rate Build. - Tracer gas dilution method* 2017.
- [35] A. Persily, L. de Jonge, Carbon dioxide generation rates for building occupants, *Indoor Air* 27 (5) (2017) 868–879.
- [36] Nordic Ventilation Group; Rehva Technology and Research Committee COVID-19 Task Force Health-based target ventilation rates and design method for reducing exposure to airborne respiratory infectious diseases. REHVA proposal for post-COVID target ventilation rates. *Rehva* 2022.
- [37] J. Wang, J. Huang, Z. Feng, S.-J. Cao, F. Haghhighat, Occupant-density-detection based energy efficient ventilation system: Prevention of infection transmission, *Energy Build.* 240 (2021), 110883.
- [38] CEN/TR Standard. 16798-4. Energy performance of buildings - Ventilation for buildings - Part 4: Interpretation of the requirements in EN 16798- 3 - For non-residential buildings. *Perform. Requir. Vent. room-conditioning Syst. M5-1, M5-4*.
- [39] ANSI/ASHRAE Standard 62.2-2022 Ventilation and Acceptable Indoor Air Quality in Residential Buildings. 2022.
- [40] G. Cao, H. Awbi, R. Yao, Y. Fan, K. Sirén, R. Kosonen, J.J. Zhang, A review of the performance of different ventilation and airflow distribution systems in buildings, *Build. Environ.* 73 (2014) 171–186.
- [41] B. Yang, A.K. Melikov, A. Kabanshi, C. Zhang, F.S. Bauman, G. Cao, H. Awbi, H. Wigö, J. Niu, K.W.D. Cheong, A review of advanced air distribution methods-theory, practice, limitations and solutions, *Energy Build.* 202 (2019), 109359.
- [42] Y. Lu, D. Niu, S. Zhang, H. Chang, Z. Lin, Ventilation indices for evaluation of airborne infection risk control performance of air distribution, *Build. Environ.* 222 (2022), 109440.

fileadmin/content/documents/Downloadable_documents/REHVA_COVID-19_Recommendation_Criteria_for_room_air_cleaners_for_particulate_matter.pdf.

- [22] Y. Guo, N. Zhang, T. Hu, Z. Wang, Y. Zhang, Optimization of energy efficiency and COVID-19 pandemic control in different indoor environments, *Energy Build.* 261 (2022), 111954.
- [23] A. Aganovic, G. Cao, J. Kurnitski, A. Melikov, P. Wargocki, Zonal modeling of air distribution impact on the long-range airborne transmission risk of SARS-CoV-2, *Appl. Math. Model.* 112 (2022) 800–821.
- [24] Coleman, K.K.; Tay, D.J.W.; Tan, K. Sen; Ong, S.W.X.; Than, T.S.; Koh, M.H.; Chin, Y.Q.; Nasir, H.; Mak, T.M.; Chu, J.J.H. Viral load of severe acute respiratory syndrome coronavirus 2 (SARS-CoV-2) in respiratory aerosols emitted by patients with coronavirus disease 2019 (COVID-19) while breathing, talking, and singing. *Clin. Infect. Dis.* 2022, 74, 1722–1728.
- [25] R. Costa, B. Olea, M.A. Bracho, E. Albert, P. de Michelena, C. Martínez-Costa, F. González-Candela, D. Navarro, RNA viral loads of SARS-CoV-2 Alpha and Delta variants in nasopharyngeal specimens at diagnosis stratified by age, clinical presentation and vaccination status, *J. Infect.* 84 (2022) 579–613.
- [26] R. Sender, Y.M. Bar-On, S. Gleizer, B. Bernshtain, A. Flamholz, R. Phillips, R. Milo, The total number and mass of SARS-CoV-2 virions, *Proc. Natl. Acad. Sci.* 118 (2021).
- [27] B. Killingley, A.J. Mann, M. Kalinova, A. Boyers, N. Goonawardane, J. Zhou, K. Lindsell, S.S. Hare, J. Brown, R. Frise, Safety, tolerability and viral kinetics during SARS-CoV-2 human challenge in young adults, *Nat. Med.* 28 (2022) 1031–1041.
- [28] B. Binazzi, B. Lanini, R. Bianchi, I. Romagnoli, M. Nerini, F. Gigliotti, R. Duranti, J. Milic-Emili, G. Scano, Breathing pattern and kinematics in normal subjects during speech, singing and loud whispering, *Acta Physiol.* 186 (2006) 233–246.
- [29] N. Van Doremalen, T. Bushmaker, D.H. Morris, M.G. Holbrook, A. Gamble, B. N. Williamson, A. Tamin, J.L. Harcourt, N.J. Thornburg, S.I. Gerber, Aerosol and surface stability of SARS-CoV-2 as compared with SARS-CoV-1, *N. Engl. J. Med.* 382 (2020) 1564–1567.
- [30] CEN EN Standard. 16798-3. Energy performance of buildings - Ventilation for buildings - Part 3: For non-residential buildings. *Perform. Requir. Vent. room-conditioning Syst. (Modules M5-1, M5-4)* 2017.
- [31] Mundt, M.; Mathisen, H.M.; Moser, M.; Nielsen, P. V Ventilation effectiveness: Rehva guidebooks. 2004.
- [32] M. Bivolarova, J. Ondráček, A. Melikov, V. Ždímal, A comparison between tracer gas and aerosol particles distribution indoors: The impact of ventilation rate, interaction of airflows, and presence of objects, *Indoor Air* 27 (2017) 1201–1212.
- [33] J. Shen, M. Kong, B. Dong, M.J. Birnkrant, J. Zhang, A systematic approach to estimating the effectiveness of multi-scale IAQ strategies for reducing the risk of airborne infection of SARS-CoV-2, *Build. Environ.* 200 (2021), 107926.
- [34] ISO/TC 163; CEN/TC 89 ISO 12569:2017 Thermal performance of buildings and materials. *Determ. Specif. airflow rate Build. - Tracer gas dilution method* 2017.
- [35] A. Persily, L. de Jonge, Carbon dioxide generation rates for building occupants, *Indoor Air* 27 (5) (2017) 868–879.
- [36] Nordic Ventilation Group; Rehva Technology and Research Committee COVID-19 Task Force Health-based target ventilation rates and design method for reducing exposure to airborne respiratory infectious diseases. REHVA proposal for post-COVID target ventilation rates. *Rehva* 2022.
- [37] J. Wang, J. Huang, Z. Feng, S.-J. Cao, F. Haghhighat, Occupant-density-detection based energy efficient ventilation system: Prevention of infection transmission, *Energy Build.* 240 (2021), 110883.
- [38] CEN/TR Standard. 16798-4. Energy performance of buildings - Ventilation for buildings - Part 4: Interpretation of the requirements in EN 16798- 3 - For non-residential buildings. *Perform. Requir. Vent. room-conditioning Syst. M5-1, M5-4*.
- [39] ANSI/ASHRAE Standard 62.2-2022 Ventilation and Acceptable Indoor Air Quality in Residential Buildings. 2022.
- [40] G. Cao, H. Awbi, R. Yao, Y. Fan, K. Sirén, R. Kosonen, J.J. Zhang, A review of the performance of different ventilation and airflow distribution systems in buildings, *Build. Environ.* 73 (2014) 171–186.
- [41] B. Yang, A.K. Melikov, A. Kabanshi, C. Zhang, F.S. Bauman, G. Cao, H. Awbi, H. Wigö, J. Niu, K.W.D. Cheong, A review of advanced air distribution methods-theory, practice, limitations and solutions, *Energy Build.* 202 (2019), 109359.
- [42] Y. Lu, D. Niu, S. Zhang, H. Chang, Z. Lin, Ventilation indices for evaluation of airborne infection risk control performance of air distribution, *Build. Environ.* 222 (2022), 109440.